Journal of Power Sources 248 (2014) 330–336

Contents lists available at ScienceDirect

Journal of Power Sources

journal homepage: www.elsevier.com/locate/jpowsour

Improved reaction kinetics and selectivity by the TiO_2-embedded carbon nanofiber support for electro-oxidation of ethanol on PtRu nanoparticles

Nobuyoshi Nakagawa [a, b, *], Yudai Ito [a], Takuya Tsujiguchi [a], Hirokazu Ishitobi [b]

[a] Department of Chemical and Environmental Engineering, Graduate School of Engineering, Gunma University, 1-5-1 Tenjin-cho, Kiryu, Gunma 376-8515, Japan

[b] Division of Environmental Engineering Science, Faculty of Science and Technology, Gunma University, 1-5-1 Tenjin-cho, Kiryu, Gunma 376-8515, Japan

HIGHLIGHTS

- PtRu/TECNF showed the highest mass activity for the ethanol electro-oxidation.
- PtRu/TECNF improved the reaction kinetics and reduced the acetic acid selectivity.
- The mass activity for the ethanol oxidation was similar to that for the methanol one.

ARTICLE INFO

Article history:
Received 5 August 2013
Received in revised form
10 September 2013
Accepted 13 September 2013
Available online 21 September 2013

Keywords:
Direct ethanol fuel cell (DEFC)
Electro-oxidation mechanism
PtRu nanoparticles
TiO_2-embedded carbon nanofiber
Reaction products
Kinetic constants

ABSTRACT

The electro-oxidation of ethanol by the catalyst of PtRu nanoparticles supported on a TiO_2-embedded carbon nanofiber (PtRu/TECNF), which has recently been proposed by the authors as a highly active catalyst for methanol oxidation, is investigated by cyclic voltammetry using a glassy carbon electrode and by operating a direct ethanol fuel cell (DEFC) with the catalyst. The mass activity obtained from the cyclic voltammogram for the ethanol oxidation is compared to that for the methanol oxidation reported in our recent paper. The mass activity for the ethanol oxidation is comparable or slightly higher than that for the methanol oxidation, and the relationship between the TECNF composition, i.e., the Ti/C mass ratio, and the activity are also similar to that for the methanol oxidation. A DEFC fabricated with the PtRu/TECNF shows a higher power output compared to that with the commercial PtRu/C catalyst. An analysis of the reaction products by a simple two-step reaction model reveals that the PtRu/TECNF increases the rate constant for the reaction steps from ethanol to acetaldehyde and subsequently to CO_2, but decreases that from acetaldehyde to acetic acid. This means that the PtRu/TECNF improves not only the kinetics, but also the selectivity to acetaldehyde.

1. Introduction

Direct ethanol fuel cells (DEFCs) have been receiving much attention as an alternative power source with a high energy density that significantly exceeds that of conventional secondary batteries. In addition, the non-toxicity of ethanol and many production routes for ethanol from various resources including biomass are advantages of the DEFC. However, the power output and the energy conversion efficiency of the current DEFCs are still low in practical use due to the high overvoltage at the electrodes. Hence, many studies have been carried out to produce an active anode catalyst for the ethanol electro-oxidation mainly focusing on Pt and Pt-based catalysts [1–19] as well as modifying the catalyst support [13,14] and co-catalyst [15–18]. For instance, secondary and ternary metal additives like Ru [2,3,5,8,9,12–14], Sn [3,4,6,9], Pd [3], Mo [2] Rh [7,12,15] and W [3,11] to Pt and Pt-based binary metals could improve the current density compared to that of only Pt.

Although many of the above studies have mainly focused on increasing the oxidation current, another important point is the product distribution that determines the energy conversion efficiency and energy density of the DEFC. Ideally, the complete oxidation of ethanol to CO_2 is desired at the anode, however, it does not easily occur at moderate temperatures under 100 °C due to the difficulty of breaking the C–C bond on the electrode.

* Corresponding author. Division of Environmental Engineering Science, Faculty of Science and Technology, Gunma University, 1-5-1 Tenjin-cho, Kiryu, Gunma 376-8515, Japan. Tel.: +81 277 30 1457; fax: +81 277 30 1458.
E-mail addresses: nakagawa@cee.gunma-u.ac.jp, nobnaka@sannet.ne.jp (N. Nakagawa).

0378-7753/$ – see front matter © 2013 Elsevier B.V. All rights reserved.
http://dx.doi.org/10.1016/j.jpowsour.2013.09.055

Table 1
Properties of the PtRu catalyst on the different supports measured by XRD and EDX [12].

Catalyst	Composition [wt%]					Pt/Ru [atm/atm]	Ti/C [wt/wt]	PtRu crystalline size [nm]	TiO_2 crystalline size [nm]
	Pt	Ru	C	Ti	O				
PtRu/C	10.2	5.7	84.2	–	–	0.93	–	9.4	–
PtRu/TiO_2	12.2	5.1	–	39.3	43.5	1.23	–	5.5	32.2
PtRu/(C + TiO_2)	9.8	5.3	55.0	13.0	16.9	0.95	0.24	6.7	40.2
PtRu/TECNF[0]	13.4	6.9	70.4	–	9.3	1.01	0.00	5.0	–
PtRu/TECNF[0.2]	13.8	7.3	57.4	9.7	11.9	0.98	0.17	5.1	62.2
PtRu/TECNF[0.4]	11.2	6.4	46.5	18.0	17.9	0.90	0.39	4.5	71.4
PtRu/TECNF [0.9]	10.2	6.6	30.8	27.2	25.3	0.80	0.88	–	–
PtRu/TECNF[1.0]	12.9	7.4	27.4	28.5	24.3	0.87	1.04	3.5	54.7
PtRu/TECNF [1.9]	10.7	7.6	18.8	35.5	27.4	0.73	1.89	3.9	71.4
PtRu/TECNF [2.6]	11.5	6.4	13.7	36.0	33.0	0.94	2.62	6.4	59.3
PtRu/C_{com}	30.0	23.3	46.7	–	–	1.29	–	3.8	–

The reaction products and the oxidation mechanism of ethanol on the electrode have been investigated by differential electrochemical mass spectroscopy (DEMS) [19–23] and/or (*in situ*) Fourier transformation infrared (FTIR) [22–25]. The measurement of the product distribution at the DEFC anode was also conducted to study the reaction mechanism [12,23,27]. Previous studies [6,12,20,21,23,25,27] revealed that the major products are usually CH_3CHO and CH_3COOH with a small amount of CO_2, except at high temperatures over 170 °C [26], and the formation of CO_2 and CH_3COOH occurs during the electro-oxidation of CH_3CHO in an acid medium [22]. Although the binary and ternary metal additions to the Pt-based catalyst enhanced the ethanol oxidation activity and/or increased the current density and then the power generation of the DEFC, most of them did not improve the CO_2 selectivity [6,12,20,21,25,27]. The decrease in the CO_2 selectivity caused an increase in the CH_3COOH selectivity [12,27]. Unfortunately, CH_3COOH formation at low temperatures is not desirable for the DEFC, because CH_3COOH is fairly resistant against the further oxidation on the Pt-based catalyst [12,21]. Therefore, a catalyst that can rapidly convert ethanol to CO_2 or CH_3CHO, but not to CH_3COOH, is preferred for the DEFC application at low temperatures.

Recently, the authors proposed PtRu nanoparticles supported on TiO_2-embedded carbon nanofibers, PtRu/TECNF, as a catalyst for the methanol electro-oxidation having a mass activity about 4 times higher than that of the conventional PtRu/C [28]. The high activity was considered to be due to the strong interaction between the metal nanoparticles and the TiO_2-embedded carbon nanofiber support. Since a positive correlation can be expected for the mass activity of the catalyst for both the methanol and ethanol oxidations, an enhanced mass activity for the ethanol oxidation can also be expected for this catalyst. It is also interesting how the effect of the TECNF support, that would induce the strong interaction between the metal and the support, affects the oxidation mechanism. Although there are some other studies employing TiO_2 as the co-catalyst of the Pt-based catalyst for the ethanol oxidation [17,18], the effect of TiO_2 on the product distribution and the reaction mechanism has not yet been investigated.

In this study, the electro-oxidation of ethanol on PtRu/TECNF was investigated by cyclic voltammetry and chronoamperometry using a glassy carbon electrode. The effect of the TECNF composition, i.e., Ti/C mass ratio, on the ethanol oxidation activity was discussed by comparing it to that for the methanol oxidation activity. Furthermore, DEFCs with the PtRu/TECNF and a commercial PtRu catalyst which is supported on carbon black, PtRu/C_{com}, were fabricated and operated, and the ethanol oxidation mechanism on the PtRu/TECNF was investigated based on the measured product distribution and a simple two-step reaction model.

2. Experimental

2.1. Preparation of the catalyst

The catalysts, PtRu nanoparticles supported on TiO_2-embedded carbon nanofibers (PtRu/TECNF), used in this study, were exactly the same as that prepared in a recent study [28]. Briefly, the preparation procedure is as follows.

A certain amount of high purity TiO_2 nanoparticles (P25, Nippon Aerosil Co., Ltd.) was dispersed into a dimethylformamide (DMF, Wako Pure Chemicals Ind., Ltd.) solution of polyacrylonitrile (PAN, Sigma–Aldrich Co., Ltd.). The mixture was then electrospun by using a setup under the optimized conditions. The obtained nanofibers were first dried in air at room temperature for 3 h and then stabilized in air at 250 °C for 10 h. The stabilized nanofibers were then carbonized in a nitrogen atmosphere at 1000 °C for 1 h followed by steam treatment with N_2, after bubbling in water at 70 °C, at 850 °C, and 200 mL min^{-1} for 1 h. Two hundred mg of the obtained nanofibers, TECNF, were then milled for 5 min to normalize the fiber length. The TECNF with different Ti/C mass ratios (=*x*) was prepared and denoted as TECNF[*x*]. The 20 wt % Pt–Ru (in an atomic ratio of 1:1) was deposited on the TECNF and the other support materials including the carbon black (C, Vulcan XC-72R), TiO_2 nanoparticles (TiO_2, P25) and the mixture of these particles (C + TiO_2) by the chemical reduction with $NaBH_4$ (Wako Pure Chemicals Ind., Ltd.) of H_2PtCl_6 (Wako Pure Chemicals Ind., Ltd.) and $RuCl_3$ (Wako Pure Chemicals Ind., Ltd.) as the precursor.

2.2. Characteristics of the catalyst

The characteristics of the prepared catalyst have been reported in a recent paper [28], and the composition determined by EDX and the crystalline size calculated from XRD are summarized in Table 1. The crystalline size of PtRu was calculated to be 4–9 nm, although a relatively large error may be included due to the broadening of the XRD peak, and that of TiO_2 was between 30 nm and 70 nm. The diameter of the TECNF was between 100 and 300 nm, and the TiO_2 in TECNF was rutile, whereas it was a mixture of anatase and rutile in the other supports. An XPS analysis showed that the surface carbon of TECNF was N-doped carbon containing a small amount of nitrogen. The morphology and structure of the TECNF were described in a previous paper [28].

2.3. Measurement of the mass activity

The ethanol oxidation activity of the prepared catalyst with the different supports was evaluated by cyclic voltammetry in a three-electrode cell with a fixed glassy carbon electrode (GCE) (3-mm

diameter) at room temperature. The catalyst ink was prepared by dispersing 5 mg of the catalyst in a mixture containing 80 μL of water, 80 μL of ethanol, and 25 μL of a 5 wt% Nafion solution (Wako Pure Chemicals Ind., Ltd.), then the mixture was ultrasonicated for 30 min. A 2.5 μL aliquot of the ink was removed using a micropipette and deposited on the glassy carbon electrodes. After the electrode was dried in air at room temperature for 1 h, it was heated in an oven at 100 °C for 30 min. A Pt wire and a mercury/mercurous sulfate electrode were used as the counter and reference electrodes, respectively. The electrolyte was a solution of 2 M ethanol containing 0.5 M H_2SO_4. After nitrogen was bubbled into the solution for 20 min to obtain an oxygen-free atmosphere near the working electrode, the CV measurement was conducted in the potential range from 0 to 1.2 V vs. NHE at the scan rate of 20 mV s^{-1} during N_2 bubbling at room temperature.

2.4. DEFC performance

The DEFC performance of the membrane electrode assembly (MEA) with PtRu/TECNF was evaluated. A certain amount of the catalyst, in the form of a slurry with 2-propanol and water, was painted on the carbon paper (TGP-H-090, Toray). This was then used as the anode after drying. The electrolyte membrane, Nafion 117 (Du Pont), was sandwiched between the anode and a commercial Pt(1.0 mg cm^{-2})/C electrode (EC-20-10, ElectroChem, Inc.) as the cathode by hot pressing them at 410 K and 5 MPa for 3 min to form the MEA. The loading of the metal catalyst for the anode of the MEA with PtRu/TECNF[0.4] and PtRu/TECNF[1.0] was 0.51 and 0.58 $mg_{\text{-PtRu}}$ cm^{-2}, respectively. The MEA with a commercial PtRu/C (PtRu/C_{com}, TEC61E54, Tanaka Kikinzoku Kogyo K.K., Pt: 30.0 wt%, Ru: 23.3 wt%), 2.06 $mg_{\text{-PtRu}}$ cm^{-2}, was also prepared and used for comparison.

The MEA was fixed in the cell holder with serpentine flow channels in both the anode and cathode (FC05–01SP, ElectroChem, Inc.), and was operated as a DEFC by pumping an aqueous ethanol solution to the anode and dry oxidant gas to the cathode at 353 K. The geometric electrode area of the DEFC was 5 cm^2.

The measurement of the current–voltage relationship and other electrochemical measurements including that for the three-electrode cell were conducted using an electrochemical measurement system (HAG-5010, Hokuto Denko, Co., Ltd.).

2.5. Analysis of the reaction products

During the power generation at a constant cell voltage, the emission from the anode outlet was collected in a bag for 2 h. The emission was a liquid without gas bubbles in this experiment. Therefore, the organic compound dissolved in the fuel and collected solution was analyzed by gas chromatography using columns of PEG6000 and an FID detector. Also, the dissolved CO_2 in the solutions was measured by a CO_2 electrode (CE-2041, DKK-TOA Corp.).

A 2-h collection was also conducted under the open circuit conditions in order to cancel the products due to oxidant crossover through the membrane. Hence, the amounts of the products were obtained by subtracting that under the open circuit condition from that under the closed circuit condition.

The chemical selectivity for component i, CS_i, was calculated based on the total amount of the reaction products at the anode, according to our previous study [12].

$$CS_i[\%] = \frac{100nM_i}{M_{CH_3CHO} + M_{CH_3COOH} + 2M_{CO_2}} \quad (1)$$

where M_i is the amount of product for component i; i.e., CH_3CHO, CH_3COOH and CO_2, and n is the coefficient which is 2 for CO_2 and 1 for the others.

3. Results and discussion

3.1. Ethanol oxidation activity of the catalysts with the different supports

Fig. 1 shows the cyclic voltammogram measured in 2 M ethanol with 0.5 M H_2SO_4 at room temperature for the PtRu catalyst prepared on the different supports; i.e., PtRu/C, PtRu/TiO_2 PtRu/CNF (PtRu/TECNF[0]) in Fig. 1(a), and PtRu/(C + TiO_2) and PtRu/TECNF [0.2] in Fig. 1(b). The ethanol oxidation activity, e.g., current density at 0.6 V vs. NHE in the forward scan, strongly depended on the support. PtRu/TiO_2 showed the worst activity, and this would be due to the very low electric conductivity of the TiO_2 particles. For the support, the TiO_2 addition to the carbon black increased the activity (i.e., the higher activity for PtRu/(C + TiO_2) compared to that for PtRu/C), and the carbon nanofiber was better than the carbon black, in addition, embedding of the TiO_2 into the carbon nanofiber further increased the activity resulting in the order; PtRu/TECNF[0.2] > PtRu/(C + TiO_2) > PtRu/CNF > PtRu/C > PtRu/TiO_2. In

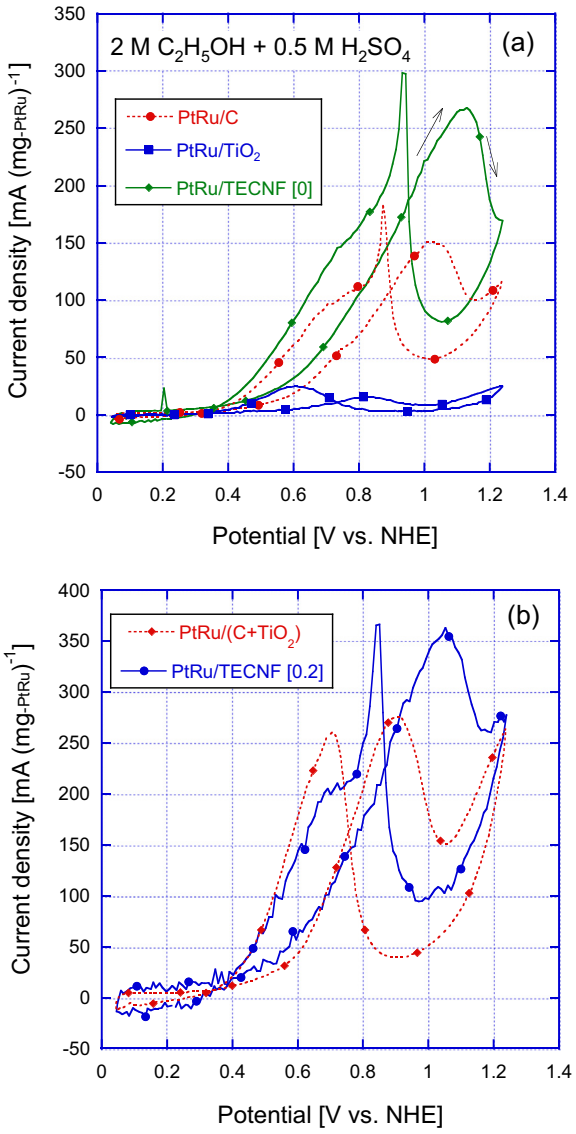

Fig. 1. Cyclic voltammograms for the PtRu catalysts prepared on different supports measured in 2 M ethanol with 0.5 M H_2SO_4 at the scan rate of 20 mV s^{-1}. (a) PtRu/C, PtRu/TiO_2, and PtRu/TECNF[0], (b) PtRu/(C + TiO_2); Ti/C = 0.24 and PtRu/TECNF; Ti/C = 0.17.

Table 2
Summary of the catalysts with the different supports in terms of mass activity, *i*, at 0.6 V vs. NHE and the peak potentials during the forward scan of the CV curve measured in 2 M C_2H_5OH + 0.5 M H_2SO_4. The summary of the catalysts measured in 2 M methanol + 0.5 M H_2SO_4 [12] is also listed for comparison.

Catalyst	Ethanol oxidation			Methanol oxidation [12]		
	$i_{0.6}$ [mA(mg_{-PtRu})$^{-1}$]	E_{peak} [*V* vs. NHE]	i_{peak} [mA (mg_{-PtRu})$^{-1}$]	$i_{0.6}$ [mA(mg_{-PtRu})$^{-1}$]	E_{peak} [*V* vs. NHE]	i_{peak} [mA (mg_{-PtRu})$^{-1}$]
PtRu/C	19	1.01	151	40	0.85	125
PtRu/TiO_2	6	0.82	16	4	0.81	9
PtRu/(C + TiO_2)	44	0.91	276	34	0.94	162
PtRu/TECNF[0]	32	1.13	268	47	0.94	202
PtRu/TECNF[0.2]	67	1.05	363	56	1.05	313
PtRu/TECNF[0.4]	62	1.05	392	87	1.01	366
PtRu/TECNF[0.9]	112	1.05	471	149	0.95	406
PtRu/TECNF[1.0]	120	1.10	604	120	1.06	516
PtRu/TECNF[1.9]	92	1.10	505	83	1.00	451
PtRu/TECNF[2.6]	74	0.93	407	50	0.89	202

the catalysts with the different supports, the mass activity and its order for the ethanol oxidation is strongly related to that for the methanol oxidation [12] as shown in Table 2, suggesting that the electro-oxidation activity of ethanol is similar and comparable to that of methanol. For the TECNF support, the effect of the Ti/C ratio on the activity is shown in Fig. 2. The Ti/C ratio in TECNF was optimized at 1.0 in which the peak current density reached 600 mA mg^{-1}_{-PtRu} which is more than 2 times higher compared to that for Ti/C = 0 as shown in Table 2, similar to the case for the methanol oxidation. When the electrochemically active surface area (ECSA) for the PtRu/TECNF[*x*] with different *x* values was compared in the previous paper, only about a 25% increase was found at the optimum Ti/C ratio compared to that of PtRu/TECNF[0], and then the increased mass activity of PtRu/TECNF[*x*] was attributed to the metal-support interaction between the PtRu nanoparticles and the TECNF support.

In Table 2, the mass activity at 0.6 V vs. NHE was almost similar in both the methanol and ethanol solutions for the same catalyst. On the other hand, the mass activity at the peak potential was slightly higher in the ethanol solution compared to that in the methanol solution. The higher current density at the peak potential for the ethanol oxidation would be due to the 1.5 times higher number of hydrogen atoms, which are easily removed and oxidized on the electrode, on an ethanol molecule compared to that on a methanol one.

Such a high mass activity of PtRu/TECNF for the ethanol oxidation suggests an expectation of a high DEFC power output comparable to a DMFC. However, it was not realized as will be mentioned below.

3.2. DEFC performance

Fig. 3 shows the DEFC performance with the PtRu/TECNF anode catalyst measured in 2 M ethanol (1.5 mL min^{-1}) and O_2 (1000 mL min^{-1}) at 353 K. In the figure, the performance of the DEFC with PtRu/C_{com} is also shown for comparison. The PtRu loading for the anode of each DEFC was different from each other, i.e., it was 0.58, 0.51 and 2.06 mg_{-PtRu} cm^{-2} for PtRu/TECNF[1.0], PtRu/TECNF[0.4] and PtRu/C_{com}, respectively. Although the PtRu loading for the PtRu/TECNF was much lower than that for the PtRu/C_{com}, the DEFC with PtRu/TECNF generated a much higher power, 9.5 mW cm^{-2} for PtRu/TECNF[1.0] or almost similar power densities, 4.2 mW cm^{-2} for PtRu/TECNF[0.4], compared to the DEFC with the PtRu/C_{com} of 4.5 mW cm^{-2} for PtRu/C_{com}, reflecting their enhanced catalytic activity by the TECNF support. On the other hand, it should be noted that the DEFC power densities were quite small, ca. one fifth, compared to that of the DMFC operated under similar conditions; 2 M methanol (1.5 mL min^{-1}) and O_2 (1000 mL min^{-1}) at 353 K [28]. In spite of the comparable or higher current densities in the cyclic voltammogram for the ethanol oxidation compared to that for the methanol oxidation as shown in Table 2, the very poor performance of the DEFC would be explained by a higher overvoltage at the cathode due to ethanol crossover [29]. In fact, it is known that the cathode performance is sensitive to

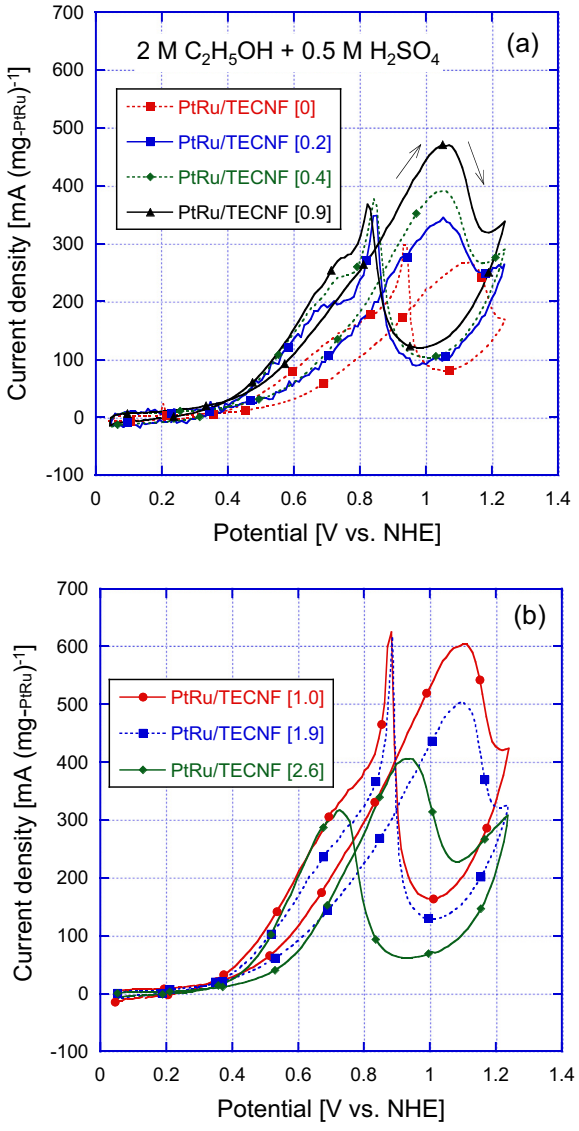

Fig. 2. Cyclic voltammograms for PtRu/TECNF with different Ti/C ratios measured in 2 M ethanol with 0.5 M H_2SO_4 at the scan rate of 20 mV s^{-1}. (a) PtRu/TECNF[*x*]; *x* = 0–0.9, (b) PtRu/TECNF[*x*]; *x* = 1.0–2.6.

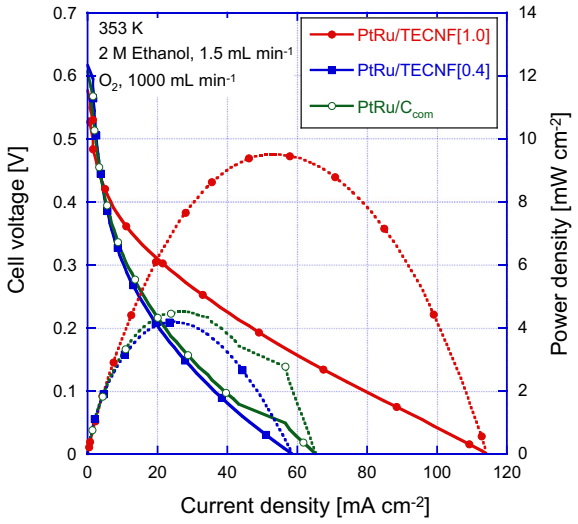

Fig. 3. Current–voltage curves for the DEFCs with PtRu/TECNF[1.0] (PtRu loading; 0.58 $mg_{\text{-PtRu}}$ cm^{-2}), that with PtRu/TECNF[0.4] (PtRu loading; 0.51 $mg_{\text{-PtRu}}$ cm^{-2}) and that with PtRu/C_{com} (PtRu loading; 2.06 $mg_{\text{-PtRu}}$ cm^{-2}), measured at 353 K in 2 M ethanol (1.5 mL min^{-1}) and dry oxygen (1 L min^{-1}).

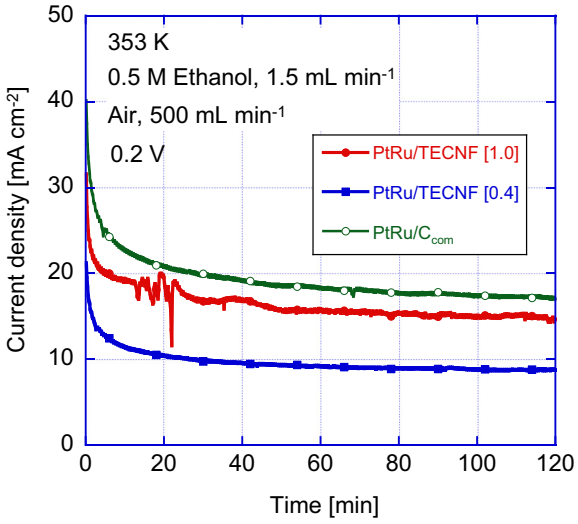

Fig. 4. Plot of current density at the constant cell voltage of 0.2 V vs. time for the DEFCs with the different anode catalysts measured at 353 K in 0.5 M ethanol (1.5 mL min^{-1}) and dry air (0.5 L min^{-1}).

the rate of ethanol crossover [30]. It should be then noted that development of a proper catalyst that is not affected by the ethanol crossover and active for the oxygen reduction activity is necessary for the DEFC [31–33].

Table 3
Production rate and the chemical selectivity for each component at the anode of the DEFC with the different catalysts operated at 353 K.

Anode catalyst	Production rate [mol $(mg_{\text{-PtRu}})^{-1}$ s^{-1}]			Chemical selectivity [%]		
	Acetaldehyde	Acetic acid	CO_2	Acetaldehyde	Acetic acid	CO_2
PtRu/TECNF[1.0]	2.95E-8	6.56E-9	5.77E-10	79.3	17.6	3.1
PtRu/TECNF[0.4]	1.28E-8	5.23E-9	1.42E-10	69.9	28.5	1.5
PtRu/C_{com}	3.29E-9	3.45E-9	9.82E-11	47.5	49.7	2.8

Fig. 4 shows the current density at a 0.2 V constant cell voltage versus time for the DEFC with the anode catalyst operating by feeding 0.5 M ethanol (1.5 mL min^{-1}) and air (500 mL min^{-1}). Since the ethanol concentration and the oxidant were different from that of Fig. 3, the order of the current density in the different catalysts was different from that of Fig. 3. The current density initially rapidly decreased, then slowly decreased, and became nearly constant. During the 2-h operation, the reaction products at the anode were collected and analyzed. The detected component was acetaldehyde, acetic acid and carbon dioxide which agreed with past studies [6,12,20,21,23,25]. The production rate and the chemical selectivity for each component during the operation in Fig. 4 are summarized in Table 3. From the table, it is found that the main product was acetaldehyde followed by acetic acid and then CO_2 according to the previous report for the PtRu/C catalyst [6,12,20,21,23,25]. It is clearly shown that the selectivity for acetic acid was strongly reduced in the case of PtRu/TECNF, while the selectivity for CO_2 was low and only a few percent irrespective of the type of catalyst. Furthermore, PtRu/TECMF[1.0] with the higher activity for the ethanol oxidation showed a lower selectivity for acetic acid compared to PtRu/TECNF[0.4]. The low selectivity for acetic acid is preferred for the DEFC because acetic acid is only slightly electro-oxidized under the typical conditions and causes degradation of the fuel cell power generation by poisoning the catalyst [12,21]. Based on these results, it was found that the catalyst support, TECNF in which the TiO_2 nanoparticles were embedded in the carbon nanofiber, affected the electro-oxidation mechanism of ethanol on PtRu.

As a reaction mechanism of the electro-oxidation of ethanol, a simple model that consists of two steps with three pathways, as shown in Fig. 5, has been proposed for the anode with Pt/C, PtRu/C and PtRuRh/C based on the power generation experiment including ethanol, acetaldehyde and acetic acid as the fuel [12].

$$C_2H_5OH \xrightarrow{k_1} CH_3CHO + 2H^+ + 2e^- \quad (2)$$

$$CH_3CHO + H_2O \xrightarrow{k_2} CH_3COOH + 2H^+ + 2e^- \quad (3)$$

$$CH_3CHO + 3H_2O \xrightarrow{k_3} 2CO_2 + 10H^+ + 10e^- \quad (4)$$

This was similar to that proposed in a previous paper [21] with the exception of the direct pathway to CO_2. In the first step, ethanol was oxidized to acetaldehyde and then further oxidized to acetic acid or carbon dioxide in the second step. Each reaction step takes place via adsorbed intermediates on the catalyst surface, and the concentration of each of the adsorbed intermediates was assumed to be in equilibrium with the product in the exhaust solution. Although the direct pathway from ethanol to CO_2 with the dissociative adsorption of ethanol was considered in previous reports [5,25,26], the direct pathway was neglected in this study according to our previous paper [12]. The direct pathway through the dissociative adsorption of ethanol to CO_2 would not be the main one under the experimental conditions in this study. Also, the pathway from acetic acid to CO_2 was denied because of the negligibly small

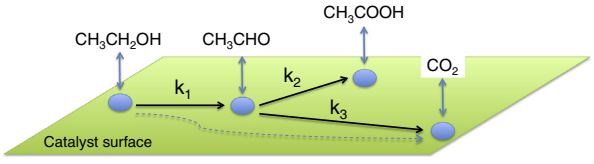

Fig. 5. Assumed reaction scheme for the ethanol oxidation on the catalyst.

current density from the acetic acid fuel as reported in a previous paper [12].

For the two-step with the three-pathway mechanism, the following kinetic equations were derived assuming that the rate of each electrochemical reaction was first order of the concentration of the related compounds;

$$r_{CH_3CHO} = \frac{dM_{CH_3CHO}}{dt} = k_1 C_{C_2H_5OH} - k_2 C_{CH_3COOH} - k_3 C_{CO_2} \quad (5)$$

$$r_{CH_3COOH} = \frac{dM_{CH_3COOH}}{dt} = k_2 C_{CH_3CHO} \quad (6)$$

$$r_{CO_2} = \frac{dM_{CO_2}}{dt} = k_3 C_{CH_3CHO} \quad (7)$$

where r_i is the production rate of component i and C_i is the concentration of component i in the bulk solution, and k is the rate constant. By applying the measured production rates and the concentrations in equations (5)–(7), the rate constants k_1–k_3 could be obtained.

Table 4 shows the calculated rate constant for each reaction step of the ethanol oxidation for the DEFC operations shown in Fig. 4. The constant k_1 is the rate constant for the reaction from ethanol to acetaldehyde. The value of k_1 for PtRu/C_{com}, 1.36E-11 m^3 $(mg_{-PtRu})^{-1}$ s^{-1}, was almost equal to that for PtRu/C, 1.46E-11 m^3 $(mg_{-PtRu})^{-1}$ s^{-1}, in a previous paper [12] suggesting that these catalytic activities are equivalent. Compared to the value of k_1 for PtRu/C_{com}, those for PtRu/TECNF[1.0] and PtRu/TECNF[0.4] were 5.4 and 2.7 times higher, respectively, according to the increased mass activity shown in Table 2. The rate constant for the reaction from acetaldehyde to CO_2, k_3, proportionally increased with k_1 showing a similar value of the k_3/k_1 ratio for the different catalysts. On the other hand, k_2, the rate constant for the reaction from acetaldehyde to acetic acid, was not proportional to k_1 and decreased by the employment of TECNF showing a similar or reduced ratio of k_2/k_1 for PtRu/TECNF compared to PtRu/C_{com}. For PtRu/TECNF[1.0], k_2 was only 1.8 times higher than that of PtRu/C_{com} while k_1 and k_3 were 5.4 times higher. This means that the formation of acetic acid was strongly restrained by the TECNF at the optimum Ti/C ratio. Since acetic acid is harmful for the Pt-based anode catalyst of the DEFC, the low selectivity for acetic acid is preferred. The PtRu/TECNF showing the advantage of the increased rate constant for k_1 and k_3, and the low selectivity for acetic acid suggested that the strong interaction between the PtRu/TECNF improves not only the kinetics, but also the reaction mechanism.

Although we showed the improved kinetics and selectivity for the electro-oxidation of ethanol on PtRu/TECNF, the CO_2 selectivity was not improved and was still low. Further studies are necessary in order to achieve a high CO_2 selectivity and enhance the kinetics. Since Pt/C is known to show a relatively high CO_2 selectivity of ca. 20–30% [12,27], Pt/TECNF can be considered as a candidate that simultaneously satisfies both the increased kinetics and CO_2 selectivity. Anyway, it was clearly shown that the support can affect both the kinetics and selectivity, thus various combinations between the metal catalyst and the support should be investigated. Additionally, an alternative cathode catalyst that is not affected by the ethanol crossover is also necessary for the high performing DEFC.

Table 4
Calculated rate constant for each step of the ethanol electro-oxidation for the DEFC performance with the different anode catalysts.

Anode catalyst	Rate constant $[m^3 (mg_{-PtRu})^{-1} s^{-1}]$			Ratio		
	k_1	k_2	k_3	k_1/k_1	k_2/k_1	k_3/k_1
PtRu/TECNF[1.0]	7.34E-11	3.24E-9	2.85E-10	1	44	3.89
PtRu/TECNF[0.4]	3.63E-11	6.57E-9	1.78E-10	1	181	4.89
PtRu/C_{com}	1.36E-11	1.84E-9	5.25E-11	1	135	3.85

4. Conclusions

The electro-oxidation of ethanol at PtRu nanoparticles prepared on the TECNF support, PtRu/TECNF, was investigated by cyclic voltammetry using a glassy carbon electrode and by operating the DEFC with the catalyst. For each PtRu catalyst, the mass activity for the ethanol electro-oxidation was comparable to that for the methanol electro-oxidation irrespective of the type of support and the Ti/C ratio in the TECNF. PtRu/TECNF showed the highest mass activity, 603 mA $(mg_{-PtRu})^{-1}$, at the Ti/C ratio of 1.0, and the DEFC with the PtRu/TECNF[1.0] generated a 2 times higher electric power with a quarter of the PtRu loading compared to that with PtRu/C_{com}. The analysis of the reaction products revealed the strongly reduced selectivity for acetic acid in the DEFC with PtRu/TECNF[1.0]. The interaction between the metal and the support of PtRu/TECNF affected not only the reaction kinetics, but also the reaction mechanism.

Acknowledgment

Part of this work was supported by the Element Innovation Project, Ministry of Education, Japan, and by the Iketani Science and Technology Foundation.

References

[1] E. Antolini, J. Power Sources 170 (2007) 1–12.
[2] Oliveira Neto, M.J. Giz, J. Perez, E.A. Ticianelli, E.R. Gonzalez, J. Electrochem. Soc. 149 (2002) A272–A279.
[3] W. Zhou, Z. Zhou, S. Song, W. Li, G. Sun, P. Tsiakaras, Q. Xin, Appl. Cat. B: Environ. 46 (2003) 273–285.
[4] C. Lamy, S. Rousseau, E.M. Belgsir, C. Coutanceau, J.-M. Léger, Electrochim. Acta 49 (2004) 3901–3908.
[5] E.V. Spinacé, A.O. Neto, M. Linardi, J. Power Sources 129 (2004) 121–126.
[6] F. Vigier, C. Coutanceau, A. Perrard, E.M. Belgsir, C. Lamy, J. Appl. Electrochem. 34 (2004) 439–446.
[7] R.T.S. Oliveira, M.C. Santos, B.G. Marcussi, S.T. Tanimoto, L.O.S. Bulhões, E.C. Pereira, J. Power Sources 157 (2006) 212–216.
[8] Z. Liu, L. Hong, J. Appl. Electrochem. 37 (2007) 505–510.
[9] A.O. Neto, R.R. Dias, M.M. Tusi, M. Linardi, E.V. Spinacé, J. Power Sources 166 (2007) 87–91.
[10] S.-B. Han, Y.-J. Song, J.-M. Lee, J.-Y. Kim, K.-W. Park, Electrochem. Comm. 10 (2008) 1044–1047.
[11] R.C.H. Maya, O.U. Reyes, J.G. Fadrique, H.C. López, P.R. Tejeda, J. Electrochem. Soc. 160 (2013) H185–H191.
[12] N. Nakagawa, Y. Kaneda, M. Wagatsuma, T. Tsujiguchi, J. Power Sources 199 (2012) 103–109.
[13] V. Bambagioni, C. Bianchini, A. Marchionni, J. Filippi, F. Vizza, J. Teddy, P. Serp, M. Zhiani, J. Power Sources 190 (2009) 241–251.
[14] J.M. Sieben, M.M.E. Duarte, Int. J. Hydrogen Energy 37 (2012) 9941–9947.
[15] G.R. Salazar-Banda, H.B. Suffredinib, L.A. Avaca, S.A.S. Machado, Mater. Chem. Phys. 117 (2009) 434–442.
[16] A. Kowal, M. Li, M. Shao, K. Sasaki, M.B. Vukmirovic, J. Zhang, N.S. Marinkovic, P. Liu, A.L. Frenkel, R.R. Adzic, Nat. Mater. 8 (2009) 325–330.
[17] P. Xiao, X. Guo, D.-J. Guo, H.-Q. Song, J. Sun, Z. Lv, Y. Liu, X.-P. Qiu, W.-T. Zhu, L.-Q. Chen, U. Stimming, Electrochim. Acta 58 (2011) 541–550.
[18] L. Yu, J. Xi, Electrochim. Acta 67 (2012) 166–171.
[19] J. Willsaw, J. Heitbaum, J. Electroanal. Chem. 194 (1985) 27–35.
[20] H. Wang, Z. Jusys, R.J. Behm, J. Power Sources 154 (2006) 351–359.
[21] V. Rao, C. Cremers, U. Stimming, L. Cao, S. Sun, S. Yan, G. Sun, Q. Xin, J. Electrochem. Soc. 154 (2007) B1138–B1147.
[22] T. Iwasita, E. Pastor, Electrochim. Acta 39 (1994) 531–537.
[23] Q. Wang, G.Q. Sun, L.H. Jiang, Q. Xin, S.G. Sun, Y.X. Jiang, S.P. Chen, Z. Jusys, R.J. Behm, Phys. Chem. Chem. Phys. 9 (2007) 2686–2696.
[24] H. Hitmi, E.M. Belgsir, J.-M. Léger, C. Lamy, Electrochim. Acta 39 (1994) 407–415.
[25] J. Shin, W.J. Tornquist, C. Korzeniewski, C.S. Hoaglund, Surf. Sci. 364 (1996) 122–130.
[26] J. Wang, S. Wasmus, R.F. Savinell, J. Electrochem. Soc. 142 (1995) 4218–4224.
[27] S. Rousseau, C. Coutanceau, C. Lamy, J.-M. Lager, J. Power Sources 158 (2005) 18–24.

[28] Y. Ito, T. Takeuchi, T. Tsujiguchi, M.A. Abdelkareem, N. Nakagawa, J. Power Sources 242 (2013) 280–288.
[29] V.A. Paganin, E. Sitta, T. Iwasita, W. Vielstich, J. Appl. Electrochem. 35 (2005) 1239–1243.
[30] G. Li, P.G. Pickup, J. Power Sources 161 (2006) 256–263.
[31] C. Lamy, A. Lima, V. LeRhun, f. Deline, C. Coutanceau, J.M. Léger, J. Power Sources 105 (2002) 283–296.
[32] F.C. Simões, P. Olivi, Electrocatalysis 1 (2010) 163–168.
[33] T. Lopes, E. Antolini, E.R. Gonzalez, Int. J. Hydrogen Energy 33 (2008) 5563–5570.